[^{99m}Tc]Oxotechnetium(V) Complexes of Amine-Amide-Dithiol Chelates with Dialkylaminoalkyl Substituents as Potential Diagnostic Probes for Malignant Melanoma

Matthias Friebe,[†] Ashfaq Mahmood,*[,†] Cristina Bolzati,[†,‡] Antje Drews,[§] Bernd Johannsen,[§] Michael Eisenhut,[||] Daniel Kraemer,[^] Alan Davison,[^] and Alun G. Jones[†]

Department of Radiology, Harvard Medical School and Brigham and Women's Hospital, Boston, Massachusetts 02115; Laboratory of Nuclear Medicine, Department of Clinical and Experimental Medicine, University of Ferrara, Ferrara 44100, Italy; Institute of Bioinorganic and Radiopharmaceutical Chemistry, Research-Center Rossendorf, Dresden, Germany; Department of Nuclear Medicine, University of Heidelberg, Heidelberg, Germany; and Department of Inorganic Chemistry, Massachusetts Institute of Technology, Cambridge, Massachusetts 02139

Received December 18, 2000

[^{99m}Tc]oxotechnetium(V) complexes of amine-amide-dithiol (AADT) chelates containing tertiary amine substituents were synthesized and shown to have affinity for melanoma. For complexation the AADT−$CH_2[CH_2]_nNR_2$ (n = 1, 2; R = Et, n-Bu) ligand was mixed with a [^{99m}Tc]-oxotechnetium(V)-glucoheptonate precursor to make the AADT−[^{99m}Tc]oxotechnetium(V) complexes in nearly quantitative yield. Structurally analogous nonradioactive oxorhenium(V) complexes were also synthesized and characterized. In vitro σ-receptor affinity measurements indicate these complexes to possess σ-affinity in the low micromolar range with K_i values in the 7.8−26.1 and 0.18−2.3 μM range for the σ_1- and σ_2-receptors, respectively. In vitro cell uptake of the ^{99m}Tc complexes in intact B16 murine melanoma cells at 37 °C after a 60-min incubation ranged from 12% for complex **2** (n = 1, R = n-Bu) to 68% for complex **4** (n = 2, R = n-Bu). In vivo evaluation of complexes **1-Tc**−**4-Tc** in the C57Bl/B16 mouse melanoma model demonstrated significant tumor localization. Complex **1-Tc** (n = 1, R = Et) displayed an in vivo tumor uptake of 7.6% ID/g at 1 h after administration with initial melanoma/blood (M/B), melanoma/spleen (M/S), and melanoma/lung (M/L) ratios >4; these ratios increased to 10.8, 10.1, and 7.3, respectively, at 6 h. While complex **3-Tc** (n = 3, R = Et) had an initial tumor uptake of 3.7% ID/g 1 h after administration with M/B, M/S, and M/L ratios >2, a greater tumor retention and slightly faster clearance from nontumor-containing organs resulted in M/B, M/S, and M/L ratios of 19.1, 19.1, and 12.7, respectively, at 6 h. The high tumor uptake and significant tumor/nontumor ratios indicate that such small technetium-99m-based molecular probes can be developed as in vivo diagnostic agents for melanoma and its metastases.

Introduction

The incidence of malignant melanoma is rising faster than that of any other cancer in the United States; it is estimated that 47 700 new cases will be diagnosed annually.[1] Global estimates of 105 000 new cases per year with 33 000 annual deaths are associated with melanoma of the skin.[1a] Since the early detection of all related metastases improves considerably the patient's prognosis,[1−3] the search for in vivo diagnostic probes is of special interest.[4−9] While an ^{18}F-labeled glucose analogue, 2-[^{18}F]fluoro-2-deoxy-D-glucose (^{18}F−FDG), is quite useful in positron-emission tomographic (PET) imaging of tumors[10] including melanoma,[11,12] a single-photon-emission computed tomographic (SPECT) radiopharmaceutical based on technetium-99m, a radioisotope with widespread availability, would provide a cost-effective means of early detection and diagnosis.

Earlier attempts at imaging melanoma with radiolabeled monoclonal antibodies[8,9] or simpler radiolabeled molecules, such as radioiodinated amino acids[4,5] or nucleic acids,[6,7] as false precursors in the melanin formation cycle were unsuccessful due to either insufficient tumor localization, low tumor/nontumor ratios,[4−9] or poor pharmacokinetics.[7,8] More recently, the use of radiolabeled peptides, such as ^{188}Re- and ^{99m}Tc-labeled melanotropin,[13,14] has generated encouraging results for in vivo melanoma scintigraphy.

The search for small radiolabeled molecular probes for in vivo scintigraphy has led to the identification of several radioiodinated benzamide derivatives including *N*-(2-diethylaminoethyl)-3-iodo-4-methoxybenzamide[15−19] (IMBA) (Figure 1). This radiolabeled benzamide displays an in vivo melanoma uptake of 6.7% injected dose (ID)/g at 60 min after administration in the C57Bl/B16 mouse melanoma model. It has also entered phase II clinical trials, providing images in patients of metastatic melanoma that are very encouraging.[16,20] In efforts to elucidate the uptake mechanism of these radiolabeled benzamides in melanoma, σ-receptors[21] have been explored, mainly because structurally similar benzamide ligands have been known to possess high affinity for σ-receptors, and σ-receptors are ex-

* Address for correspondence: Harvard Medical School, Department of Radiology, Goldenson Building B-1/251, 220 Longwood Avenue, Boston, Massachusetts, 02115. Tel: (617)-432-3995. Fax: (617)-432-2419. E-mail: amahmood@hms.harvard.edu.
[†] Harvard Medical School and Brigham and Women's Hospital.
[‡] University of Ferrara.
[§] Institute of Bioinorganic and Radiopharmaceutical Chemistry.
[||] University of Heidelberg.
[^] Massachusetts Institute of Technology.

10.1021/jm0005407 CCC: $20.00
Published on Web 08/15/2001

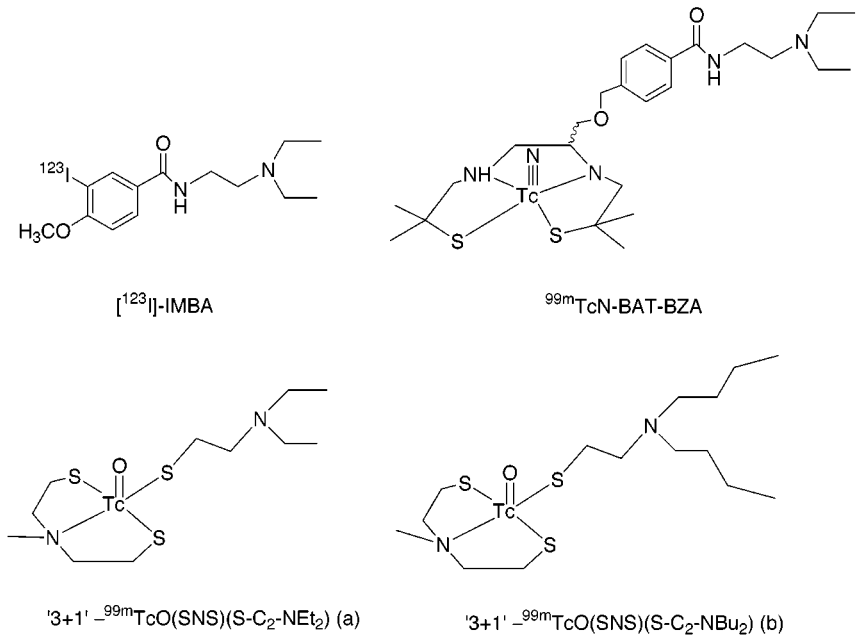

Figure 1. Iodine-123-labeled *N*-(2-diethylaminoethyl)-3-iodo-4-methoxybenzamide ([^{123}I]IMBA), technetium-99m-labeled oxotechnetium-bis-aminethiol-*N*-(2-diethylaminoethyl)benzamide ([^{99m}Tc]TcN−BAT−BZA), and two "3 + 1" oxotechnetium complexes with pendent amine groups [^{99m}Tc]TcO(SNS)(S−C_2−NEt_2) (a) and [^{99m}Tc]TcO(SNS)(S−C_2−NBu_2) (b).

pressed on a number of tumor-cell types including melanoma.[22−25] However, recent investigations have shown that the accumulation of these radiolabeled benzamides by melanoma cells is not correlated with their σ-affinity but rather with their melanin content.[18,19]

While iodine-123 can be obtained commercially, technetium-99m is available on demand through a ^{99}Mo/^{99m}Tc generator. The technetium-99m isotope emits single γ-photons of 140 keV, has a high photon flux, and decays with a 6-h half-life, making it very cost-effective and the radiolabel of choice for routine clinical SPECT imaging. Technetium-99m-labeled complexes based on the complete *N*-(2-dialkylaminoalkyl)benzamide core, such as nitridotechnetium-bis-aminethiol-benzamide (TcN−BAT−BZA) (Figure 1) have been reported with a maximum tumor uptake of 1.6% ID/g at 60 min after administration in the mouse melanoma model.[26,27] More recently, we have reported "3 + 1" mixed-ligand ^{99m}Tc complexes[28,29] that integrate the radiometal within the pharmacophore by replacing the aromatic ring with a tridentate/monodentate chelated mono-oxometal. These "3 + 1" complexes, TcO(SNS)(S−C_2−NEt_2) and TcO(SNS)(S−C_2−NBu_2) (Figure 1, a and b), display a significantly higher tumor accumulation of 3.1% and 5% ID/g, respectively, 60 min after administration. While these "3 + 1" mixed-ligand complexes[28] are easy to synthesize, their known tendency to form transchelation products with glutathione in vivo[28,30] may hamper their use as diagnostic probes.

A tetradentate chelate that replaces the aromatic moiety in the analogous benzamides would furnish the required stability and, thus, might provide higher in vivo tumor uptake. Using the tetradentate amine-amide-dithiol (AADT) chelate,[31,32] which lacks the *gem*-dimethyl groups compared with the earlier bis-aminethiol chelates and forms stable mono-oxotechenetium complexes with reduced lipophilicity, we synthesized new ^{99m}Tc complexes that may serve as potential diagnostic probes with affinity for malignant melanoma. Herein, we describe the synthesis and characterization of these tertiary-amine-bearing ^{99m}Tc−AADT complexes and their in vivo evaluation in a melanoma tumor model.

Results and Discussion

Chemistry. The N_2S_2–AADT chelate was synthesized via multistep reactions (Scheme 1) as previously described.[31,32] Chelate derivatives containing the C_2-linked dialkylamino groups as substituents (**1**, **2**) were synthesized via *N*-alkylation of the amine nitrogen in the AADT chelate using *N*-(2-dialkylamino)ethyl chloride (alkyl = Et, Bu), while the C_3-linked dialkylamino substituents (**3**, **4**) were incorporated in the chelate via alkylation of commercially available dialkylamines (alkyl = Et, Bu) using an *N*-(3-chloropropyl)−AADT derivative.[32]

Technetium-99m-labeled complexes (**1-Tc**−**4-Tc**) were synthesized by transmetalation of technetium-99m from a prereduced ^{99m}Tc−glucoheptonate precursor (Scheme 1). Upon heating the reaction mixture at 70 °C, ligand exchange of the N_2S_2−AADT ligand bearing the pendent tertiary amines and the ^{99m}Tc(V)−glucoheptonate precursor yielded complexes **1-Tc**−**4-Tc** in nearly quantitative yields within 30 min. Typical mass amounts of the ^{99m}Tc complexes preclude their physical characterization; however, since both technetium and rhenium form structurally identical AADT complexes,[32] analogous nonradioactive rhenium complexes were synthesized (vide infra) and used as surrogates for HPLC comparisons. Identical HPLC retention times established the existence of the proposed technetium-99m species.

Using a method similar to that for ^{99m}Tc complexes, the mono-oxorhenium(V) complexes **1-Re**−**4-Re** were obtained by reduction of perrhenate(VII) with stannous chloride in the presence of sodium glucoheptonate and the deprotected N_2S_2-chelating ligand; heating the reac-

Scheme 1. Synthesis of the *A*mine-*A*mide-*D*ithiol (AADT) Ligands **1**−**4** and Complexes[a]

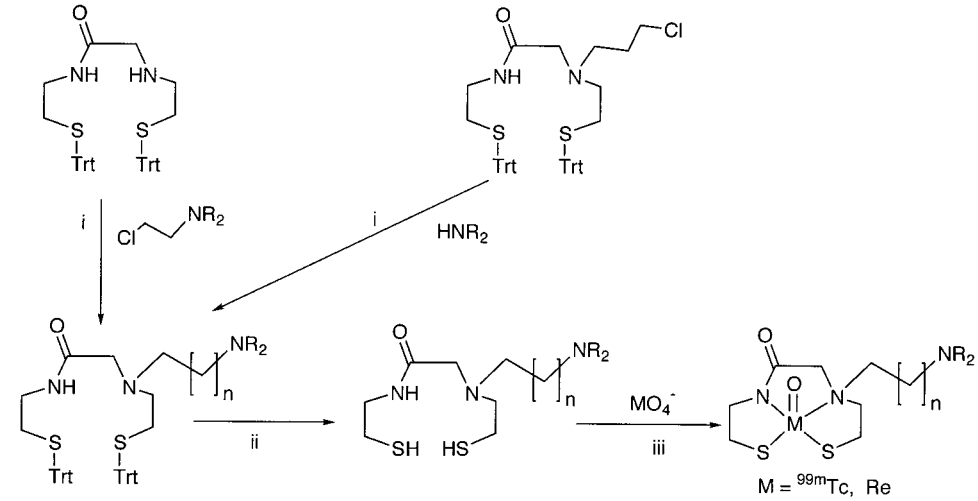

Compound	n	R
1	1	Ethyl
2	1	Butyl
3	2	Ethyl
4	2	Butyl

Complex	n	R
1-Tc/Re	1	Ethyl
2-Tc/Re	1	Butyl
3-Tc/Re	2	Ethyl
4-Tc/Re	2	Butyl

[a] (i) CH_3CN, KI, K_2CO_3, reflux, 24 h; (ii) TFA, Et_3SiH, 2 min; (iii) sodium glucoheptonate, $SnCl_2$, 75 °C, 1 h.

tion mixture at 75 °C for 1 h afforded brownish-purple solids of the rhenium complexes (**1-Re**−**4-Re**). These complexes show distinct $\upsilon_{Re=O}$ infrared vibrations in the 950−960 cm^{-1} region, typical for mono-oxorhenium complexes. Upon chelation the N-substituent on the chelate may adopt a syn or anti configuration with respect to the asymmetric M═O core. The deshielding, anisotropic environment of the M═O core and the proximity of the N-substituent in the syn configuration to the asymmetric oxometal core result in a downfield shift of the proton resonances syn to the M═O core, thus permitting differentiation of the syn and anti diastereomers via NMR.[33−36] For example, in the ^{1}H NMR of the **1-Re** complex, the methylene protons of the N-substituent (C_7) appear as two separate multiplets (doublets of doublets) downfield at 4.55 and 4.06 ppm, indicating a syn configuration of the N-substituent. This resonance pattern is also observed for the other complexes synthesized.

Further confirmation of the syn configuration was obtained by the crystal structure determination of **1-Re**. As expected, the structure displays a distorted square-pyramidal geometry, with the amine-amide-dithiol donor set forming the base-plane and the oxo group at the apex of the pyramid (Figure 2). The rhenium atom lies slightly above the AADT base-plane. The pendent tertiary amine group connected by the C_2 alkyl chain is oriented syn to the M═O core. Selected bond lengths and angles are listed in Table 1. While only the geometric syn isomer is formed, due to the presence of a stereogenic center at the substituted amine in the chelate, these complexes exist as enantiomeric pairs of two mirror images. Since most of the physiochemical parameters (vide infra) are not expected to be significantly different for the individual enantiomers, these were not separated further and are used as such.

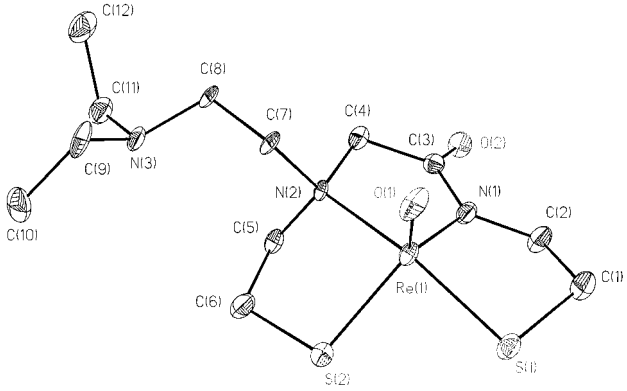

Figure 2. Crystal structure of [ReOAADT]−C_2−NEt_2 (**1**).

Table 1. Selected Bond Length and Angles of Complex **1-Re**

bond length (Å)		bond angle (deg)	
Re(1)−O(1)	1.691(8)	O(1)−Re(1)−N(1)	118.1(4)
Re(1)−N(1)	1.977(10)	O(1)−Re(1)−N(2)	101.6(4)
Re(1)−N(2)	2.172(9)	N(1)−Re(1)−N(2)	79.9(4)
Re(1)−S(2)	2.268(3)	O(1)−Re(1)−S(2)	116.7(3)
Re(1)−S(1)	2.275(3)	N(1)−Re(1)−S(2)	124.9(3)
S(1)−C(1)	1.847(13)	N(2)−Re(1)−S(2)	83.8(2)
S(2)−C(6)	1.835(12)	O(1)−Re(1)−S(1)	106.2(3)
O(2)−C(3)	1.190(14)	N(1)−Re(1)−S(1)	82.6(3)
N(2)−C(4)	1.50(2)	N(2)−Re(1)−S(1)	151.7(3)
N(2)−C(5)	1.50(2)	S(2)−Re(1)−S(1)	88.17(11)
N(2)−C(7)	1.55(2)	C(4)−N(2)−Re(1)	109.1(7)

The physicochemical parameters of the rhenium complexes, i.e., lipophilicity log *P*, log $D_{pH7.4}$, and pK_a (Table 2) were determined using HPLC methods.[37−39] As expected, the dibutylamine group in **2-Re** (C_2-linked) displays a higher log *P* of 3.3 compared with the diethylamine-containing complex **1-Re** (C_2-linked), which has a log *P* of 1.6. Although the dibutyl groups in **2-Re** would normally lead to a more basic amine moiety

Table 2. pK_a, Lipophilicity, RP-HPLC Retention Time, and σ_1- and σ_2-Receptor Affinity for the Oxorhenium(V) AADT Complexes

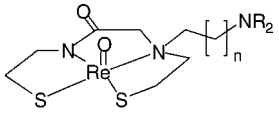

complex	n	R	pK_a	$D_{pH7.4}$	log $D_{pH7.4}$	P	log P	RP-HPLC t_R (min)	K_i (μM) σ_1[a]	K_i (μM) σ_2[b]
1-Re	1	ethyl	7.7	14	1.1	38.7	1.6	30.6	10.9 ± 2.4	2.3 ± 0.3
2-Re	1	*n*-butyl	7.7	80	1.9	2186	3.3	39.5	nd[c]	nd
3-Re	2	ethyl	9.2	0.3	−0.5	19.2	1.3	35.8	26.1 ± 3.3	0.18 ± 0.04
4-Re	2	*n*-butyl	9.5	5	0.7	1349	3.1	40.2	7.8 ± 7.0	1.6 ± 0.25

[a] Determined in guinea pig brain homogenate; radioligand, [^{3}H]-(+)-pentazocine. [b] Determined in rat liver homogenate; radioligand, [^{3}H]DTG in the presence of 1 μM dextrallorphan to mask σ_1-receptors. [c] None detected.

compared with **1-Re**, both complexes have a pK_a = 7.7. Since log $D_{pH7.4}$ is a composite measure of log P and pK_a, the log $D_{pH7.4}$ of **2-Re** (1.9) is also higher than that of **1-Re** (1.1). A similar log P difference is found for the C_3-linked complexes **3-Re** and **4-Re**. However, unlike **1-Re** and **2-Re**, the dibutylamine complex **4-Re** yields a slightly higher pK_a of 9.5 compared with 9.2 for the diethylamine complex **3-Re**. The log P of the C_3-linked complexes **3-Re** and **4-Re** is slightly lower than those of the C_2-linked analogues **1-Re** and **2-Re**. With pK_a values >9 for complexes **3-Re** and **4-Re**, the resulting low log $D_{pH7.4}$ values of −0.5 (**3-Re**) and 0.7 (**4-Re**) are not surprising, since the complexes would exist in a protonated form at pH 7.4.

In Vitro Tumor-Uptake Studies. Tumor-cell uptake studies in B16/F0 murine melanoma cells were performed with complexes **1-Tc**−**4-Tc** at 37 and 4 °C. Additionally, tumor-cell uptake of complex **1-Tc** and **3-Tc** were investigated in another rapidly dividing MCF-7 human breast cancer cell line.

All compounds display a rapid cell uptake within 10 min of incubation at 37 °C (Figure 3a,b). While the C_2-linked complex **1-Tc** (R = Et) has a maximal cell uptake of 43%, its slightly less lipophilic C_3 analogue **3-Tc** (R = Et) has a higher uptake of 62%. With the more lipophilic dibutyl homologues, the C_3-linked complex **4-Tc** (R = Bu) has the highest melanoma cell uptake of 68%, and its corresponding C_2 analogue (R = Bu) the lowest of the entire test set (12%).

To distinguish an active uptake component from passive diffusion, measurements were also carried out at 4 °C. A decrease in the incubation temperature from 37 to 4 °C results in a lower cell uptake for complexes **1-Tc**, **3-Tc**, and **4-Tc** (Figure 3a,b), with the most lipophilic complex **4-Tc** showing the least difference (23% decrease) and the least lipophilic complex **3-Tc** the greatest difference (77% decrease). To ensure that the decreased uptake at 4 °C is due to decreased metabolism and not cell death, the tumor cells were reincubated at 37 °C for 60 min following a 4 °C incubation; this restored the tumor-cell uptake of the complexes to the level observed at 37 °C (data not shown). These observations indicate a significant active accumulation process occurring for these compounds in melanoma cells. It is presumably the presence of this active component in the cell-uptake process at 37 °C that makes it difficult to deduce any correlations with either lipophilicity (log P and log $D_{pH7.4}$) or in vivo tumor uptake of these complexes.

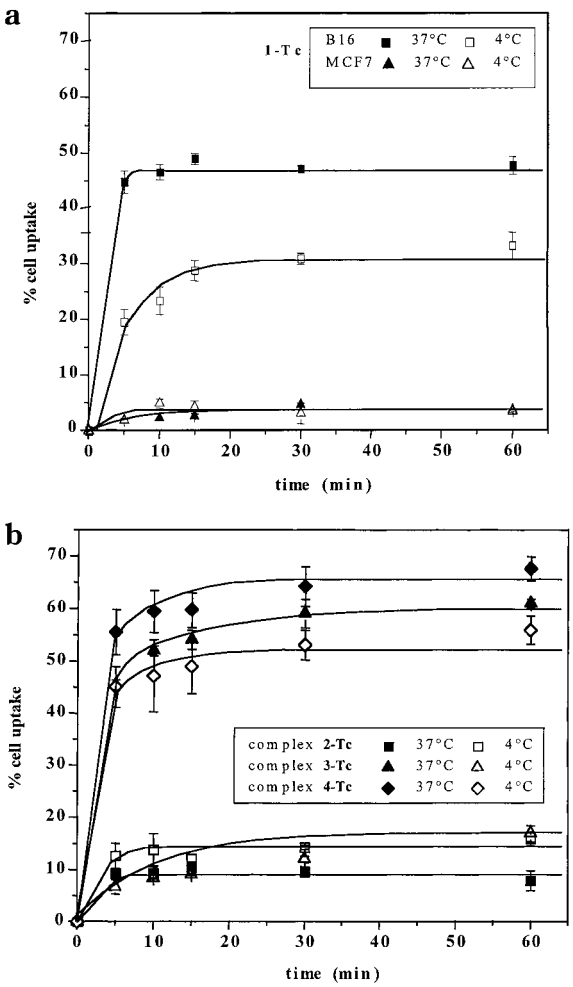

Figure 3. In vitro cell uptake of complex **1-Tc** (a) and complexes **2-Tc**−**4-Tc** (b) in B16 murine melanoma and MCF-7 human breast cancer (5×10^6 cells/mL) at 37 and 4 °C.

The in vitro uptake of complex **2-Tc** is unexpectedly low for reasons not yet understood. However, complex **2-Tc** exhibits the highest log P (3.3) among the four complexes and also a pK_a of 7.7, making it very lipophilic at pH 7.4, as indicated by its log $D_{pH7.4}$ of 1.9, which may contribute to this unusual behavior. The tumor-cell uptake of complex **1-Tc** in another rapidly dividing tumor-cell line MCF-7 has a maximum cell uptake of only 6% at 37 °C compared with 43% for the B16/F0 cell line (Figure 3a). Additionally, complex **3-Tc** displays only a 17% maximal uptake at 37 °C in the MCF-7 cell line (data not shown) compared with the 62% maximal uptake in the B16 melanoma cell line.

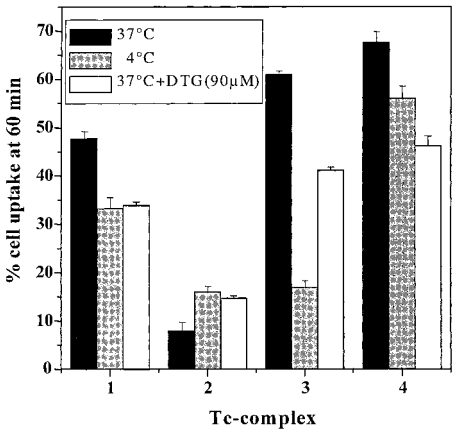

Figure 4. In vitro cell uptake at 1 h of complexes **1-Tc**−**4-Tc** in B16 murine melanoma cells (5×10^6 cells/mL) incubated at 37 and 4 °C, and 37 °C with DTG (90 μM).

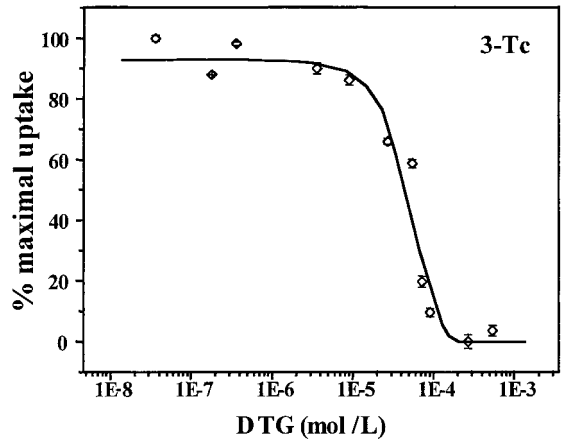

Figure 5. Dose-dependent uptake inhibition of **3-Tc** with DTG (90 μM) in B16 melanoma cells (5×10^6 cells/mL) at 37 °C.

Since the radioiodinated benzamides have been reported to possess high affinity for σ-receptors expressed by various tumors,[22−25] tumor-cell uptake studies of the complexes were also performed in the presence of 1,3-di-*o*-tolylguanidine (DTG), a known high-affinity σ-ligand. Preincubation of the tumor cells with DTG (90 μM), 30 min prior to the uptake experiments with the ^{99m}Tc complexes, yields a lower tumor-cell uptake for complexes **1-Tc** (29% less), **3-Tc** (33% less), and **4-Tc** (32% less) at 37 °C (Figure 4). Additional dose−response experiments conducted with intact B16/F0 cells at 37 °C with **3-Tc** and DTG as the inhibitor (Figure 5) show a DTG-concentration-dependent decrease in the uptake of the complex. Complexes **1-Tc**, **3-Tc**, and **4-Tc** exhibit 50% maximal inhibition at 21, 49, and 52 μM DTG, respectively.

Receptor-Binding Studies. To gain a better understanding of the involvement of σ-receptor binding in the melanoma-cell uptake of these ^{99m}Tc complexes, we further investigated the affinity of these complexes in an established σ-receptor assay. Employing the structurally similar nonradioactive rhenium complexes **1-Re**, **3-Re**, and **4-Re** as surrogates for the ^{99m}Tc complexes, competitive binding assays were carried out with guinea pig brain membranes (σ_1-receptors) and rat liver membranes (σ_2-receptors) to assess σ-receptor subtype selectivity, while [^{3}H]-(+)-pentazocine[40] (σ_1) and [^{3}H]DTG/dextrallorphan[41] (σ_2) were used as high-affinity radioligands. The apparent K_d values for the radioligands are 6.44 ± 0.53 nM (σ_1) and 23.7 ± 2.0 nM (σ_2), respectively. All four Re complexes display only micromolar affinity toward the σ_1-receptor (Table 2). In general, their K_i (σ_1) values range from 7.8 to 26.1 μM. However, unlike the iodobenzamides,[19,22] all four complexes have a slightly higher affinity for the σ_2-receptor compared with the σ_1-receptor (Table 2). The K_i values for the σ_2-receptor range from 0.18 to 2.3 μM with **3-Re** displaying 100-fold greater affinity toward the σ_2-receptor subtype.

The apparent low σ-receptor affinity of **1-Re**−**4-Re**; the low tumor-cell uptake of these compounds in MCF-7 cells, known to express σ_2 receptors;[22,24] and the high micromolar concentrations of DTG required to inhibit the tracer concentration of the ^{99m}Tc complex uptake in intact B16 melanoma cells would seem to suggest that, while binding to the σ-receptors cannot be excluded from the accumulation process, the inhibitory effects observed in the intact B16 cell-uptake assay may be due to secondary effects induced by DTG on the growth and proliferation of the B16 melanoma cells.[42,43] Other factors such as melanin production and content may play a more significant role in the accumulation of these complexes in melanomas, as recently shown with the radioiodinated benzamides.[18,19]

In Vivo Tumor Uptake. To study the tumor uptake of ^{99m}Tc complexes **1-Tc**−**4-Tc** in vivo, biodistribution experiments at 1 and 6 h after their administration were carried out in C57Bl6 mice with palpable B16 melanoma nodules. The biodistribution data including melanoma/nontumor (M/NT) ratios for selected organs are summarized in Table 3 as percentage injected dose per gram (% ID/g).

Complex **1-Tc** (C_2-linked, R = Et) displays the highest tumor uptake of the entire test set with 7.6% ID/g and high melanoma/blood (M/B) (7.6), melanoma/spleen (M/S) (4.2), and melanoma/lung (M/L) (5.4) ratios at 1 h after administration. Although the % ID/g in the tumor decreases at 6 h after administration (3.5% ID/g), the M/NT ratios increase for blood (10.8), spleen (10.1), and lung (7.3) due to the faster clearance of the complex from these tissues compared with the tumor. In comparison, complex **2-Tc** (C_2-linked, R = *n*-Bu), the more lipophilic analogue (log $D_{pH7.4}$ = 1.9), has a lower melanoma uptake of 3.0% ID/g 1 h after administration. While the total tumor uptake is significantly lower than that for **1-Tc**, the M/NT ratios are equivalent (except for a lower M/L value of 2.1) at the 1-h time point. At 6 h after administration, although the M/NT ratios increase, the lower tumor content of complex **2-Tc** (1.1% ID/g) may be inadequate for in vivo imaging.

Complex **3-Tc** (C_3-linked, R = Et) has a melanoma uptake of 3.7% ID/g at 1 h after administration and M/NT ratios almost identical to those for complexes **1-Tc** and **2-Tc** (except for M/L). However, a greater retention in tumor tissue and a faster clearance from nontumor tissues result in a significant increase in the M/NT ratios for **3-Tc** at the 6-h point, giving M/B, M/S, and M/L ratios of 19, 19, and 12.7, respectively. The melanoma uptake of complex **4-Tc** (1.3% ID/g 1 h after administration) and the M/NT ratios are the lowest of the test set and may be far from ideal for in vivo diagnostic purposes.

Table 3. Biodistribution and Tumor/Nontumor Ratios of Complexes **1-Tc**−**4-Tc** at 1 and 6 h Postinjection[a]

	1-Tc		2-Tc		3-Tc		4-Tc	
organ	1 h	6 h	1 h	6 h	1 h	6 h	1 h	6 h
blood	1.00[b] ± 0.46	0.32 ± 0.19	0.39 ± 0.07	0.13 ± 0.01	0.48 ± 0.10	0.14 ± 0.05	0.31 ± 0.10	0.09 ± 0.02
heart	0.82 ±0.37	0.11 ± 0.02	0.32 ±0.20	0.07 ± 0.04	0.38 ± 0.29	0.02 ± 0.01	0.27 ± 0.15	0.04 ± 0.01
lung	1.40 ± 0.49	0.47 ± 0.21	1.39 ± 0.45	0.27 ± 0.12	1.55 ± 0.79	0.21 ± 0.04	0.86 ± 0.35	0.24 ± 0.13
spleen	1.83 ± 0.55	0.34 ± 0.10	0.73 ± 0.16	0.17 ± 0.01	1.24 ± 0.33	0.14 ± 0.06	0.92 ± 0.26	0.34 ± 0.02
liver	12.7 ± 1.54	4.08 ± 0.92	10.9 ± 0.57	5.66 ± 0.53	14.6 ± 1.88	6.42 ± 1.12	6.83 ± 0.96	2.45 ± 1.12
kidney	5.53 ± 0.81	1.98 ± 0.21	6.78 ±1.12	3.30 ± 0.52	5.62 ± 0.41	2.97 ± 0.41	3.49 ± 0.60	2.00 ± 0.86
muscle	0.35 ± 0.21	0.08 ± 0.01	0.98 ± 0.34	0.06 ± 0.03	0.38 ± 0.14	0.06 ± 0.02	0.13 ± 0.03	0.05 ± 0.02
brain	0.30 ± 0.10	0.05 ± 0.02	0.16 ± 0.08	0.01 ± 0.01	0.08 ± 0.01	0.01 ± 0.01	0.04 ± 0.01	0.01 ± 0.00
melanoma	7.62 ± 0.62	3.45 ± 1.2	2.95 ± 0.23	1.14 ± 0.26	3.70 ± 0.32	2.67 ± 0.29	1.31 ± 0.17	0.80 ± 0.29
mel/blood	7.6 ± 0.54	10.8 ± 1.00	7.6 ± 0.33	8.8 ± 0.32	7.7 ± 0.43	19.1 ± 0.33	4.2 ± 0.21	8.9 ± 0.10
mel/spleen	4.2 ± 0.58	10.1 ± 1.11	4.0 ± 0.80	6.7 ± 0.24	3.0 ± 0.30	19.1 ± 0.28	1.4 ± 0.34	2.4 ± 0.09
mel/lung	5.4 ± 0.60	7.3 ± 0.98	2.1 ± 0.81	4.2 ± 0.22	2.4 ± 1.00	12.7 ± 0.22	1.5 ± 0.41	3.3 ± 0.16
mel/liver	0.6 ± 0.09	0.9 ± 0.35	0.3 ± 0.03	0.2 ± 0.18	0.3 ± 0.08	0.4 ± 0.2	0.2 ± 0.15	0.3 ± 0.19

[a] $n = 4$ animals per time point. [b] Values represent % ID/g wet tissue.

Similar to our earlier results with the "3 + 1" complexes,[29] a log $D_{pH7.4} = 1$ seems to favor a higher melanoma uptake of these ^{99m}Tc complexes. However, unlike the "3 + 1" complexes, where p$K_a = 9.9$ gives the highest melanoma uptake, the more rigid tetradentate ^{99m}Tc−AADT complexes, such as **1-Tc** with p$K_a = 7.7$, display a higher in vivo melanoma uptake.

The exact tumor-uptake mechanism of these complexes still remains unclear. The higher in vivo tumor accumulation of the relatively more stable tetradentate AADT complexes (relative to the "3 + 1" complexes) suggests a more specific involvement of intramolecular processes than simple entrapment due to instability of the complex or its transmetalation to intracellular proteins.

Conclusions

Integrating the radiometal within the pharmacophore of melanoma-targeting dialkylaminoethyl benzamides, such as IMBA, by replacing the aromatic ring with an oxometal−AADT moiety leads to metal complexes that display significant in vivo melanoma accumulation. Similar to the earlier oxometal "3 + 1" complexes,[29] these oxotechnetium(V)− and oxorhenium(V)−AADT complexes also contain pendent tertiary amines, and those with a log $D_{pH7.4} \approx 1$ (complex **1-Tc**) display relatively high in vivo melanoma accumulation. While the σ-receptor affinity for all the complexes is low to moderate, in vitro cell-uptake measurements indicate an active uptake component in B16 melanoma cells. The relatively high in vivo melanoma uptake coupled with the high melanoma/nontumor ratios displayed by these technetium complexes indicates that technetium-based small molecular probes that target melanoma may be designed and could potentially be useful in the early detection and diagnosis of melanoma and its metastases.

Experimental Section

All chemicals and reagents, purchased from commercial sources (Aldrich Chemicals, Gibco Life Technologies), were of analytical grade and were used without further purification. Technetium-99m pertechnetate was obtained via a generator (DuPont). Elemental analyses were performed on an elemental analyzer LECO-CHNS-932. ^{1}H NMR spectra were recorded on a Varian XL500 MHz instrument. X-ray crystallography was performed on a Siemens platform goniometer with a CCD detector using a Mo Kα radiation source. The structure was solved by direct methods using SHELXTL version 5.0. FT-IR spectra were recorded on a Bruker Vector 22 FTIR instrument with an ATR accessory. Mass spectra were obtained on a MicroMass LCZ electrospray LC-MS instrument. HPLC purification was performed on a Waters Millennium Chromatography System equipped with a 996 UV−Vis diode-array detector attached in series to a γ-detector consisting of a shielded photomultiplier powered by a Canberra voltage amplifier and connected to a ratemeter. For the purification of all complexes, a reversed-phase C_8 column equipped with a C_{18} guard was eluted with methanol (solvent A) and 0.005 M phosphate-buffered saline, pH 7.4, (Sigma) (solvent B) using a linear gradient from 15/85 (A/B) to 90/10 (A/B) at a 1.0 mL/min flow rate.

The tetradentate chelating ligand *N*-[2-((2-(S-(triphenylmethyl)thio)ethyl)amino)acetyl]-S-(triphenylmethyl)-2-aminoethanethiol (AADT-(Trt)$_2$) and the *N*-[(3-chloropropyl)-*N*-2-(2-((S-(triphenylmethyl)thio)ethyl)amino)acetyl]-S-(triphenylmethyl)-2-aminoethanethiol (AADT-(Trt)$_2$-*N*-$CH_2CH_2CH_2Cl$) derivative were synthesized as described earlier.[31,32]

Ligand Synthesis. *N*-[(2-Diethylaminoethyl)-*N*-(2-(2-(S-(triphenylmethyl)thio)ethyl)amino)acetyl]-S-(triphenylmethyl)-2-aminoethanethiol [AADT-(Trt)$_2$-*N*-CH_2CH_2-N(CH_2CH_3)$_2$] (1). *N*-(2-Diethylamino)ethyl chloride (68.8 mg, 0.4 mmol), AADT-(Trt)$_2$ (252 mg, 0.4 mmol), KI (199.2 mg, 1.2 mmol), and K_2CO_3 (276.4 mg, 2 mmol) were added to 50 mL of CH_3CN, and the solution was refluxed under argon atmosphere for 24 h. After cooling to room temperature, the inorganic salts were filtered, and the filtrate was evaporated to dryness. The residue was redissolved in CH_2Cl_2 and extracted with a basic aqueous solution (pH 11). The CH_2Cl_2 portion was evaporated to a minimum volume and chromatographed on a silica gel column with the following sequence of eluents: 100 mL of CH_2Cl_2, 200 mL of 1% CH_3OH/CH_2Cl_2, and 200 mL of 2% CH_3OH/CH_2Cl_2. TLC (SiO_2): 7% NH_3/CH_3OH (5% NH_4OH in CH_3OH)/93% CH_2Cl_2. The product was isolated as a yellow viscous oil (42% yield): ^{1}H NMR ($CDCl_3$) δ 7.946 (t, 1H, −NH), 7.435−7.208 (m, 30H, Ar), 3.116−3.077 (q, 2H, $-CH_2-$), 2.94 (s, 2H, $-CH_2CO$), 2.52−2.45 (m, 10H, $-CH_2-$), 2.403 (t, 2H, $-CH_2-$), 2.295 (t, 2H, $-CH_2-$), 0.977 (t, 6H, $-CH_3$); MS (MW = 777.4) observed 778 $(M + H)^+$. Anal. ($C_{50}H_{55}N_3OS_2$)·$^1/_2H_2O$ calcd (found): C, 76.29 (76.10); H, 7.17 (7.04); N, 5.33 (5.34).

***N*-[(2-Dibutylaminoethyl)-*N*-(2-(2-(S-(triphenylmethyl)-thio)ethyl)amino)acetyl]-S-(triphenylmethyl)-2-aminoethanethiol [AADT-*N*-CH_2CH_2-N(C_4H_9)$_2$] (2).** This compound was synthesized with *N*-(2-dibutylamino)ethyl chloride and AADT-(Trt)$_2$ using a procedure analogous to that described above for **1**. Purification was carried out on a silica gel TLC plate that was developed in 7% methanolic NH_3 (5% NH_4OH in CH_3OH)/93% CH_2Cl_2. The product was obtained as a yellowish viscous oil (38% yield): ^{1}H NMR ($CDCl_3$) δ 7.829−7.745 (s, 1H, −NH), 7.440−7.350 (m, 12H, Ar), 7.295−7.242 (m, 12H, Ar), 7.230−7.100 (m, 6H, Ar), 3.090−3.035 (q, 2H, $-CH_2-$), 2.929 (s, 2H, $-CH_2CO$), 2.540−2.300 (m, 12H, $-CH_2-$), 2.297−2.265 (m, 2H, $-CH_2-$), 1.360 (brs, 4H, $-CH_2-$), 1.285−1.220 (m, 4H, $-CH_2-$), 0.894 (t, 6H, $-CH_3$); MS (MW

= 833.2) observed 834 (M + H)$^+$. Anal. ($C_{54}H_{63}N_3OS_2$) calcd (found): C, 77.75 (77.03); H, 7.61 (7.62); N, 5.04 (5.03).

***N*-[(3-Diethylaminopropyl)-*N*-(2-(2-(S-(triphenylmethyl)thio)ethyl)amino)acetyl]-S-(triphenylmethyl)-2-aminoethanethiol [AADT-*N*-$CH_2CH_2CH_2$-$N(CH_2CH_3)_2$] (3).** AADT-*N*-$CH_2CH_2CH_2Cl$[32] (310 mg, 0.4 mmol), diethylamine (59.9 mg, 0.4 mmol), KI (340.1 mg, 2.1 mmol), and K_2CO_3 (141.7 mg, 1.0 mmol) were added to 50 mL of CH_3CN, and the solution was refluxed for 24 h. The product was purified via silica gel chromatography with 3% methanolic NH_3 (5% NH_4-OH in CH_3OH)/97% CH_2Cl_2, yielding a yellowish oil (72% yield): ^{1}H NMR ($CDCl_3$) δ 7.535−7.500 (m, 1H, −NH), 7.465−7.380 (m, 12H, Ar), 7.330−7.250 (m, 12H, Ar), 7.250−7.190 (m, 6H, Ar), 3.100−3.020 (q, 2H, $-CH_2-$), 2.896 (s, 1H, $-CH_2$-CO), 2.600−2.520 (m, 4H, $-CH_2-$), 2.500−2.400 (m, 6H, $-CH_2-$), 2.410−2.340 (m, 2H, $-CH_2-$), 2.325−2.226 (m, 2H, $-CH_2-$), 1.620−1.540 (m, 2H, $-CH_2-$), 1.025 (t, 6H, $-CH_3$); MS (MW = 791.4) observed 792 (M + H)$^+$. Anal. ($C_{51}H_{57}N_3$-OS_2)·$^1/_2H_2O$ calcd (found): C, 76.5 (76.65); H, 7.3 (7.24); N, 5.24 (5.30).

***N*-[(3-Dibutylaminopropyl)-*N*-(2-(2-(S-(triphenylmethyl)thio)ethyl)amino)acetyl]-S-(triphenylmethyl)-2-aminoethanethiol [AADT-*N*-$CH_2CH_2CH_2$-$N(C_4H_9)_2$] (4).** Dibutylamine (149.9 mg, 1.2 mmol), AADT-*N*-$CH_2CH_2CH_2Cl$[32] (584 mg, 0.8 mmol), KI (664 mg, 4 mmol), and K_2CO_3 (552.8 mg, 4.0 mmol) were dissolved in 50 mL of argon-saturated CH_3-CN and refluxed for 24 h. The product was purified via silica gel chromatography using as eluent 4% CH_3OH/96% CH_2Cl_2, followed by 10% CH_3OH/90% CH_2Cl_2, yielding a yellowish oil (78% yield): ^{1}H NMR ($CDCl_3$) δ 7.460−7.440 (m, 1H, −NH), 7.410−7.360 (m, 12H, Ar), 7.300−7.180 (m, 18H, Ar), 3.040−3.010 (q, 2H, $-CH_2-$), 2.893 (s, 2H, $-CH_2-$), 2.650−2.295 (m, 13H, $-CH_2-$), 1.900−1.380 (m, 7H, $-CH_2-$), 1.330−1.250 (m, 4H, $-CH_2-$), 0.914 (t, 6H, $-CH_3$); MS (MW = 847.5) observed 848 (M + H)$^+$. Anal. ($C_{55}H_{65}N_3OS_2$)·$^1/_2H_2O$ calcd (found): C, 77.06 (77.08); H, 7.75 (7.81); N, 4.90 (5.11).

General Procedure for Deprotection of Thiol Groups. The bis-trityl-protected AADT ligand (6.0 mg) was dissolved in 3 mL of trifluoroacetic acid (TFA) and stirred at room temperature for 5 min. The solution was titrated with triethylsilyl hydride until the disappearance of the yellow color. The TFA was evaporated completely and the dry residue was placed under high vacuum overnight. The resulting white solid was redissolved in 300 μL of argon-saturated methanol and portioned into six vials using 50-μL aliquots. The contents of the vials were then evaporated and the vials stored under vacuum for subsequent labeling with technetium-99m.

Technetium-99m Labeling (1-Tc−4-Tc). One milligram of thiol-deprotected ligand (**1**−**4**) (vide supra) dissolved in 0.25 mL of phosphate buffer (0.005 M, pH 7.4) and the required activity of ^{99m}Tc−glucoheptonate were placed in a vial, and the reaction mixture was heated at 60−75 °C for 45 min. HPLC evaluation of the ^{99m}Tc complexes typically showed 85−98% radiochemical yield. Coinjection of the characterized rhenium complexes with the analogous ^{99m}Tc complexes showed coelution of the radioactive species with the corresponding UV-active rhenium complex.

General Procedure for Rhenium Complexation. The bis-trityl-protected ligand (**1**−**4**) (100 mg, 0.1 mmol) was dissolved in 0.25 mL of anisol and 10 mL of TFA. The resulting yellow solution was stirred for 5 min and then titrated with triethylsilyl hydride until colorless. The solution was evaporated and the residue placed under high vacuum until completely dry. The residue was redissolved in 5 mL of argon-saturated 20% CH_3OH/water solution. To this was added an aqueous solution of $NaReO_4$ (30 mg, 0.1 mmol), sodium glucoheptonate (55 mg, 0.2 mmol), and solid $SnCl_2$ (21 mg, 0.1 mmol) with stirring. The solution began to turn brownish purple. The pH of the reaction mixture was adjusted to 7, and the reaction was heated at 75 °C for 1 h. The solution was then cooled to room temperature, the pH adjusted to 8, and the solution extracted with CH_2Cl_2. The extract was concentrated and chromatographed on silica gel, eluting with 4−5% CH_3OH/95% CH_2Cl_2 to yield the desired product as a pale purple solid.

[ReOAADT]-C_2-NEt_2 (1-Re): yield 74.4%; ^{1}H NMR ($CDCl_3$) δ 4.943 (d, 1H, $-CH_2CO$), 4.554 (dd, 1H, $-CH_2-$), 4.248 (d, 1H, $-CH_2CO$), 4.065 (dd, 1H, $-CH_2-$), 3.993 (m, 1H, $-CH_2-$), 3.639 (m, 1H, $-CH_2-$), 3.532 (dd, 1H, $-CH_2-$), 3.419 (ddd, 1H, $-CH_2-$), 3.212 (ddd, 1H, $-CH_2-$), 3.160 (ddd, 1H, $-CH_2-$), 2.868 (dd, 2H, $-CH_2-$), 2.795 (m, 1H, $-CH_2-$), 2.570 (m, 4H, $-CH_2-$), 1.579 (ddd, 1H, $-CH_2-$), 1.060 (t, 6H, $-CH_3$); IR $\upsilon_{Re=O}$ = 952 cm^{-1}; MS (MW = 493.1) observed 494 (M + H)$^+$. Anal. ($C_{12}H_{24}N_3O_2ReS_2$) calcd (found): C, 29.3 (29.5); H, 4.9 (5.1); N, 8.5 (8.4); S, 13.0 (12.6).

[ReOAADT]-C_2-NBu_2 (2-Re): yield 15%; ^{1}H NMR ($CDCl_3$) δ 4.963 (d, 1H, $-CH_2CO$), 4.582 (dd, 1H, $-CH_2-$), 4.209 (d, 1H, $-CH_2CO$), 4.089 (dd, 1H, $-CH_2-$), 3.975 (m, 1H, $-CH_2-$), 3.646 (m, 1H, $-CH_2-$), 3.492 (d, 1H, $-CH_2-$), 3.426 (m, 1H, $-CH_2-$), 3.264 (m, 1H, $-CH_2-$), 3.180 (m, 1H, $-CH_2-$), 2.899 (m, 2H, $-CH_2-$), 2.805 (m, 1H, $-CH_2-$), 2.464 (m, 4H, $-CH_2-$), 1.606 (m, 1H, $-CH_2-$), 1.450 (m, 4H, $-CH_2-$), 1.336 (m, 4H, $-CH_2-$), 0.943 (t, 6H, $-CH_3$); IR $\upsilon_{Re=O}$ = 958 cm^{-1}; MS (MW = 549.1) observed 550 (M + H)$^+$. Anal. ($C_{16}H_{32}N_3O_2$-ReS_2) calcd (found): C, 35.0 (34.9); H, 5.9 (5.7); N, 7.7 (7.7); S, 11.6 (11.9).

[ReOAADT]-C_3-NEt_2 (3-Re): yield 70.4%; ^{1}H NMR ($CDCl_3$) δ 4.694 (d, 1H, $-CH_2CO$), 4.567 (dd, 1H, $-CH_2-$), 4.113 (d, 1H, $-CH_2CO$), 4.081 (dd, 1H, $-CH_2-$), 4.000 (ddd, 1H, $-CH_2-$), 3.610 (ddd, 1H, $-CH_2-$), 3.399 (ddd, 1H, $-CH_2-$), 3.239 (m, 2H, $-CH_2-$), 3.184 (4d, 1H, $-CH_2-$), 2.866 (dd, 1H, $-CH_2-$), 2.555 (m, 4H, $-CH_2-$), 2.496 (m, 2H, $-CH_2-$), 1.921 (m, 2H, $-CH_2-$), 1.614 (ddd, 1H, $-CH_2-$), 1.030 (t, 6H, $-CH_3$); IR $\upsilon_{Re=O}$ = 955 cm^{-1}; MS (MW = 507.1) observed 508 (M + H)$^+$. Anal. ($C_{13}H_{26}N_3O_2ReS_2$) calcd (found): C, 30.8 (30.7); H, 5.2 (5.0); N, 8.3 (8.6); S, 12.6 (12.3).

[ReOAADT]-C_3-NBu_2 (4-Re): yield 12.4%; ^{1}H NMR ($CDCl_3$) δ 4.698 (d, 1H, $-CH_2CO$), 4.564 (dd, 1H, $-CH_2-$), 4.122 (d, 1H, $-CH_2CO$), 4.071 (dd, 1H, $-CH_2-$), 3.985 (ddd, 1H, $-CH_2-$), 3.624 (ddd, 1H, $-CH_2-$), 3.351 (ddd, 1H, $-CH_2-$), 3.268 (m, 2H, $-CH_2-$), 3.202 (4d, 1H, $-CH_2-$), 2.875 (dd, 1H, $-CH_2-$), 2.525 (m, 4H, $-CH_2-$), 2.512 (m, 2H, $-CH_2-$), 1.974 (m, 2H, $-CH_2-$), 1.645 (ddd, 1H, $-CH_2-$), 1.389 (m, 4H, $-CH_2-$), 0.94 (t, 6H, $-CH_3$); IR $\upsilon_{Re=O}$ = 956 cm^{-1}; MS (MW = 563.2) observed 564 (M + H)$^+$. Anal. ($C_{17}H_{34}N_3O_2ReS_2$) calcd (found): C, 36.2 (36.3); H, 6.1 (6.2); N, 7.5 (7.8); S, 11.4 (11.5).

X-ray Structure Determination: formula, $C_{12}H_{24}N_3O_2$-ReS_2; formula weight, 493.1; unit cell dimensions, a = 6.8929(8) Å, b = 9.8926(12) Å, c = 12.2566(14) Å, α = 93.074(2)°; β = 93.770(2)°; γ = 103.706(2)°; density, 2.025 mg/m^3 (calculated); space group, P; wavelength, 0.71073 Å; reflections, 3246 (collected), 2265 (independent); absorption correction, semiempirical from ψ-scans; refinement, full-matrix least-squares on F^2; final R indices [$I > 2\sigma(I)$], $R1$ = 0.0550, $wR2$ = 0.1361 (Supporting Information).

Determination of Lipophilicity and pK_a Values. The lipophilicity and pK_a values of all complexes were determined using HPLC methods described previously.[38,39] log P, log $D_{pH7.4}$, and pK_a values were determined on a Perkin-Elmer HPLC system 1020 using a reversed phase PRP-1 column (250 × 4.1 mm; 10 μm; Hamilton) run under isocratic conditions with a flow rate of 1.5 mL/min at room temperature. The mobile phase was acetonitrile/phosphate buffer (0.01 M), 3/1, with the aqueous buffer adjusted to the desired pH between 3 and 11.[38,39] The capacity factor (k') was calculated for each determination[37,44] and the partition coefficient at a given pH (D or log D) was calculated from the equation: log $D = a$ log $k' + b$, where the parameters a and b are predetermined using standard amines. The fitted points of inflection from the sigmoidal D_{HPLC}/pH profiles permit calculation of the pK_{HPLC}.[38] The aqueous ionization constants pK_a were calculated from the pK_{HPLC} values after correction with a predetermined correction factor obtained using standard amine compounds. log P values of the neutral complexes were estimated from the upper plateau of the respective sigmoidal log D/pH curves in the alkaline range.

In Vitro Cell Studies. Murine B16/F0 melanoma cells and human MCF-7 breast cancer cells were obtained from American Type Culture Collection (ATCC, Manassas, VA) and were grown in T-175 flasks in 14 mL of Dulbecco's Modified Eagle Medium (D-MEM; Gibco, Life Technology, Gaithersburg, MD) containing 4500 mg/L D-glucose, L-glutamine, and pyridoxine hydrochloride, 110 mg/L sodium pyruvate, 10% fetal bovine serum (FBS), 0.2% gentamicin, and 0.5% penicillin−streptomycin solution. All cells were harvested from cell culture flasks by trypsinization with 1 mL of trypsin−EDTA solution (0.25% trypsin, 1 mM EDTA · 4 Na) (Gibco). After being washed with 12 mL of Dulbecco's phosphate-buffered saline (PBS), pH 7.2 (Ca^{2+}- and Mg^{2+}-free; g/L KCl, 0.20; KH_2PO_4, 0.20; NaCl, 8.00; Na_2HPO_4, 1.15) (Gibco), the cells were counted and resuspended in 8 mL of S-MEM (Gibco) (Ca^{2+}-free, with reduced Mg^{2+}content) and stored at 4 °C until use.

For in vitro tumor-cell accumulation studies, 5×10^6 cells in polypropylene test tubes were incubated at 37 or 4 °C, with intermittent agitation with 1−2 μCi (5 μL) ^{99m}Tc complex (**1-Tc**−**4-Tc**) in a total volume of 350 μL of S-MEM. At appropriate time intervals, the tubes were vortexed and 8-μL samples were layered on 350 μL of cold FBS in a 400-μL Eppendorf microcentrifuge tube. After centrifugation at 15 000 rpm for 2 min, the tubes were frozen in a dry ice−acetone bath. While still frozen, the bottom tip of the microcentrifuge tube containing the cell pellet was cut and placed in a counting tube. The remaining portion of the tube with the supernatant was placed in a separate counting tube. Both fractions were counted for radioactivity in a γ-counter (WALLAC, 1480 WIZARD 3″). The amount of supernatant in the cell pellet was determined to be <1% in separate experiments. The percentage cell uptake of the ^{99m}Tc complex was calculated as % uptake = [cpm (pellet)]/[cpm (pellet) + cpm (supernatant)] × 100.

The effect of the inhibitor DTG on cell uptake of these complexes was studied by addition of the inhibitor at various concentrations to the cell suspension 30 min prior to addition of the ^{99m}Tc complexes. Fresh DTG stock solutions were made by dissolving DTG (3.0 mg, 12.5 μmol) in 0.38 mL of PBS and 0.12 mL of hydrochloric acid (0.1 N) and subjecting the mixture to ultrasound until a clear solution was obtained, followed by the addition of 0.50 mL of FBS to produce a neutral solution with pH 7.4. The stock solutions were diluted by an appropriate amount of S-MEM, and aliquots between 5 and 25 μL were added to the cell suspension such that the final concentration of DTG was between 0.02 and 120 μM in a total cell suspension volume of 350 μL.

***σ_1*-Receptor-Binding Assay.** The in vitro σ_1-binding affinities of complexes **1-Re**, **3-Re**, and **4-Re** were determined in a competition assay using guinea pig brain membranes and the high-affinity σ_1-ligand [^{3}H]-(+)-pentazocine.[40] The membranes were prepared from guinea pig brain (minus cerebellum) as previously described.[40] Fifteen concentrations of the nonradioactive rhenium complexes ranging from 1×10^{-10} to 1×10^{-3} M and protein samples (0.15 mg of membrane protein) were incubated with 5 nM [^{3}H]-(+)-pentazocine in a total volume of 0.25 mL of Tris-HCl (50 mM), pH 8. Incubations were carried out for 120 min at 25 °C. All assays were terminated by dilution with 5 mL of ice-cold Tris-HCl (10 mM), pH 8.0, and the solutions were filtered through glass-fiber filters (Whatman GF/B; presoaked in 0.5% polyethyleneimine for 30 min at 25 °C). Filters were then washed twice with 5 mL of ice-cold Tris-HCl (10 mM), pH 8.0, and counted in Hionic-Fluor cocktail (Packard, Groningen, The Netherlands). The corresponding IC_{50} values were determined with SigmaPlot software (SigmaPlot 4.0; SPSS Inc., Chicago, IL) and were used for the calculation of the apparent K_i values with the Cheng−Prusoff equation.[45]

***σ_2*-Receptor-Binding Assay.** Rat liver membranes were prepared from male Sprague−Dawley rat livers as previously described.[41] The σ_2-receptors were labeled as described[41] using [^{3}H]DTG as radioligand in the presence of 1 μM dextrallorphan to mask σ_1-receptors. Competition assays were performed with fifteen concentrations of the nonradioactive rhenium complexes ranging from 1×10^{-10} to 1×10^{-3} M and protein samples (0.15 mg of membrane protein) in Tris-HCl (50 mM), pH 8.0, for 120 min at 25 °C in a 0.25-mL volume. All other manipulations and data analysis were performed as described vide supra for the σ_1-receptor assay.

Animal Studies. All animal experiments were performed in compliance with the *Principles of Laboratory Animal Care* (NIH publication #85-23, revised 1985). Biodistribution studies and tumor-uptake measurements were performed in C57Bl6 mice (15−20 g) bearing the B16/F0 murine melanoma on the hind limb.[15,17,18,20] The tumor cells (B16/F0), obtained from ATCC, were washed with PBS and transplanted subcutaneously on the left hind flank by an inoculation of 0.5×10^6 cells (0.1 mL). Ten to 14 days later the animals developed palpable tumor nodules 3−5 mm in diameter. The biodistribution studies were carried out by tail-vein injection of 25−30 μCi (0.05−0.1 mL) of the ^{99m}Tc-labeled complexes **1-Tc**−**4-Tc**. At the designated time after tail-vein administration, the animals were weighed and sacrificed. The organs and tumors were harvested and, when appropriate, blotted dry, weighed, and counted in a γ-counter along with technetium-99m standards of the injected dose. The results are expressed as % ID/g tissue (Table 3).

Supporting Information Available: ORTEP drawing of **1-Re**, crystal data and refinement parameters, coordinates, anisotropic temperature factors, bond lengths and angles, hydrogen coordinates, and observed and calculated structure factors. This material is available free of charge via the Internet at http://pubs.acs.org.

References

(1) (a) Parkin, D. M.; Pisani, P.; Ferlay, J. Global Cancer Statistics, *CA Cancer J. Clin.* **1999**, *49*, 33−64. (b) Rigel, D. S.; Carucci, J. A. Malignant Melanoma: Prevention, Early Detection, and Treatment in the 21st Century. *CA Cancer J. Clin.* **2000**, *50*, 215−236.

(2) Devesa, S. S.; Blot, W. J.; Stone, B. J.; Miller, B. A.; Tarone, R. E.; Fraumeni, J. F., Jr. Recent Cancer Trends in the United States. *J. Natl. Cancer Inst.* **1995**, *87*, 175−182.

(3) Marks, R. An Overview of Skin Cancers: Incidence and Causation. *Cancer* **1995**, *75*, 607−612.

(4) Kloss, G.; Leven, M. Accumulation of Radioiodinated Tyrosine Derivatives in the Adrenal Medulla and in Melanomas. *Eur. J. Nucl. Med.* **1979**, *4*, 179−186.

(5) Bubeck, B.; Eisenhut, M.; Heimke, U.; zum Winkel, K. Melanoma Affine Radiopharmaceuticals. I. A Comparative Study of ^{131}I-Labeled Quinoline and Tyrosine Derivatives. *Eur. J. Nucl. Med.* **1981**, *6*, 227−233.

(6) Larsson, B.; Olander, K.; Dencker, L.; Holmqvist, L. Accumulation of ^{125}I-Labelled Thiouracil and Propylthiouracil in Murine Melanotic Melanomas. *Br. J. Cancer* **1982**, *46*, 538−550.

(7) van Langevelde, A.; Bakker, C. N. M.; Broxterman, H. J.; Journée-de Korver, J. G.; Kaspersen, F. M.; Oosterhuis, J. A.; Pauwels, E. K. J. Potential Radiopharmaceuticals for the Detection of Ocular Melanoma. Part I. 5-Iodo-2-thiouracil Derivatives. *Eur. J. Nucl. Med.* **1983**, *8*, 45−51.

(8) Buraggi, G. L.; Callegaro, L.; Mariani, G.; Turrin, A.; Cascinelli, N.; Attili, A.; Bombardieri, E.; Terno, G.; Plassio, G.; Dovis, M.; Mazzuca, N.; Natali, P. G.; Scassellati, G. A.; Rosa, U.; Ferrone, S. Imaging with ^{131}I-Labeled Monoclonal Antibodies to a High-Molecular-Weight Melanoma-Associated Antigen in Patients with Melanoma: Efficacy of Whole Immunoglobulin and Its F(ab′)$_2$ Fragments. *Cancer Res.* **1985**, *45*, 3378−3385.

(9) Larson, S. M. Biologic Characterization of Melanoma Tumors by Antigen-Specific Targeting of Radiolabeled Anti-tumor Antibodies. *J. Nucl. Med.* **1991**, *32*, 287−291.

(10) Delbeke, D. Oncological Applications of FDG PET Imaging: Brain Tumors, Colorectal Cancer, Lymphoma, and Melanoma. *J. Nucl. Med.* **1999**, *40*, 591−603.

(11) Macfarlane, D. J.; Sondak, V.; Johnson, T.; Wahl, R. L. Prospective Evaluation of 2-[^{18}F]-2-Deoxy-D-glucose Positron Emission Tomography in Staging of Regional Lymph Nodes in Patients with Cutaneous Malignant Melanoma. *J. Clin. Oncol.* **1998**, *16*, 1770−1776.

(12) Ruhlmann, J.; Oehr, P.; Stegemann, G.; Steen, K.; Menzel, C.; Biersack, H. J. FDG-PET Compared to Conventional Diagnostic Methods in Malignant Melanoma. *J. Nucl. Med.* **1999**, *40*, 20P.

(13) Giblin, M. F.; Jurisson, S. S.; Quinn, T. P. Synthesis and Characterization of Rhenium-Complexed α-Melanotropin Analogs. *Bioconjugate Chem.* **1997**, *8*, 347−353.

(14) (a) Chen, J. Q.; Wang, N.; Jurisson, S. S.; Quinn, T. P. Biodistribution Properties of Linear and Cyclic ^{99m}Tc Labeled Alpha-Melanotropin Peptides. In *Technetium, Rhenium and Other Metals in Chemistry and Nuclear Medicine 5*; Nicolini, M., Mazzi, U., Eds.; Servizi Grafici Editoriali: Padova, 1999; pp 457−463. (b) Chen, J. Q.; Cheng, Z.; Hoffman, T. J.; Jurisson, S. S.; Quinn, T. P. Melanoma-Targeting Properties of ^{99m}Technetium-Labeled Cyclic α-Melanocyte-Stimulating Hormone Peptide Analogues. *Cancer Res.* **2000**, *60*, 5649−5658.

(15) (a) Brandau, W.; Niehoff, T.; Pulawski, P.; Jonas, M.; Dutschka, K.; Sciuk, J.; Coenen, H. H.; Schober, O. Structure Distribution Relationship of Iodine-123-Iodobenzamides as Tracers for the Detection of Melanotic Melanoma. *J. Nucl. Med.* **1996**, *37*, 1865−1871. (b) Mohammed, A.; Nicholl, C.; Titsch, U.; Eisenhut, M. Radioiodinated *N*-(Alkylaminoalkyl)-Substituted 4-Methoxy-, 4-Hydroxy-, and 4-Aminobenzamides: Biological Investigations for the Improvement of Melanoma-Imaging Agents. *Nucl. Med. Biol.* **1997**, *24*, 373−380.

(16) Nicholl, C.; Mohammed, A.; Hull, W. E.; Bubeck, B.; Eisenhut, M. Pharmacokinetics of Iodine-123-IMBA for Melanoma Imaging. *J. Nucl. Med.* **1997**, *38*, 127−133.

(17) Titsch, U.; Mohammed, A.; Wagner, S.; Oberdorfer, F.; Eisenhut, M. Syntheses of N-(2-Diethylaminoethyl)benzamides Suitable for ^{99m}Tc Complexation. *J. Labelled Compd. Radiopharm.* **1997**, *40*, 416−418.

(18) Dittmann, H.; Coenen, H. H.; Zölzer, F.; Dutschka, K.; Brandau, W.; Streffer, C. In Vitro Studies on the Cellular Uptake of Melanoma Imaging Aminoalkyl-iodobenzamide Derivatives (ABA). *Nucl. Med. Biol.* **1999**, *26*, 51−56.

(19) Eisenhut, M.; Hull, W. E.; Mohammed, A.; Mier, W.; Lay, D.; Just, W.; Gorgas, K.; Lehmann, W. D.; Haberkorn, U. Radioiodinated *N*-(2-Diethylaminoethyl)benzamide Derivatives with High Melanoma Uptake: Structure−Affinity Relationships, Metabolic Fate, and Intracellular Localization. *J. Med. Chem.* **2000**, *43*, 3913−3922.

(20) Michelot, J. M.; Moreau, M. F. C.; Veyre, A. J.; Bonafous, J. F.; Bacin, F. J.; Madelmont, J. C.; Bussiere, F.; Souteyrand, P. A.; Mauclaire, L. P.; Chossat, F. M.; Papon, J. M.; Labarre, P. G.; Kauffmann, Ph.; Plagne, R. J. Phase II Scintigraphic Clinical Trial of Malignant Melanoma and Metastases with Iodine-123-N-(2-Diethylaminoethyl 4-Iodobenzamide). *J. Nucl. Med.* **1993**, *34*, 1260−1266.

(21) Walker, J. M.; Bowen, W. D.; Walker, F. O.; Matsumoto, R. R.; de Costa, B.; Rice, K. C. Sigma Receptors: Biology and Function. *Pharmacol. Rev.* **1990**, *42*, 355−402.

(22) John, C. S.; Bowen, W. D.; Saga, T.; Kinuya, S.; Vilner, B. J.; Baumgold, J.; Paik, C. H.; Reba, R. C.; Neumann, R. D.; Varma, V. M.; McAfee, J. G. A Malignant Melanoma Imaging Agent: Synthesis, Characterization, in Vitro Binding and Biodistribution of Iodine-125-(2-Piperidinylaminoethyl)4-iodobenzamide. *J. Nucl. Med.* **1993**, *34*, 2169−2175.

(23) John, C. S.; Baumgold, J.; Vilner, B. J.; McAfee, J. G.; Bowen, W. D. [^{125}I]N-(2-Piperidinylaminoethyl)4-iodobenzamide and Related Analogs as Sigma Receptor Imaging Agents; High Affinity Binding to Human Malignant Melanoma and Rat C6 Glioma Cell Lines. *J. Labelled Compd. Radiopharm.* **1994**, *35*, 242−244.

(24) Vilner, B. J.; John, C. S.; Bowen, W. D. Sigma-1 and Sigma-2 Receptors Are Expressed in a Wide Variety of Human and Rodent Tumor Cell Lines. *Cancer Res.* **1995**, *55*, 408−413.

(25) John, C. S.; Vilner, B. J.; Gulden, M. E.; Efange, S. M. N.; Langason, R. B.; Moody, T. W.; Bowen, W. D. Synthesis and Pharmacological Characterization of 4-[^{125}I]-*N*-(*N*-Benzylpiperidin-4-yl)-4-iodobenzamide: A High Affinity σ Receptor Ligand for Potential Imaging of Breast Cancer. *Cancer Res.* **1995**, *55*, 3022−3027.

(26) Auzeloux, P.; Papon, J.; Masnada, T.; Borel, M.; Moreau, M.-F.; Veyre, A.; Pasqualini, R.; Madelmont, J.-C. Synthesis and Biodistribution of Technetium-99m-Labelled *N*-(Diethylaminoethyl)benzamide via a Bis(Dithiocarbamate) Nitridotechnetium-(V) Complex. *J. Labelled Compd. Radiopharm.* **1999**, *42*, 325−335.

(27) Auzeloux, P.; Papon, J.; Azim, E. M.; Borel, M.; Pasqualini, R.; Veyre, A.; Madelmont, J.-C. A Potential Melanoma Tracer: Synthesis, Radiolabeling, and Biodistribution in Mice of a New Nitridotechnetium Bis(Aminothiol) Derivative Pharmacomodulated by a *N*-(Diethylaminoethyl)benzamide. *J. Med. Chem.* **2000**, *43*, 190−198.

(28) Spies, H.; Pietzsch, H. J.; Johannsen, B. The "n+1" Mixed-Ligand Approach in the Design of Specific Technetium Radiopharmaceuticals: Potentials and Problems. In *Technetium, Rhenium and Other Metals in Chemistry and Nuclear Medicine 5*; Nicolini, M., Mazzi, U., Eds.; Servizi Grafici Editoriali: Padova, 1999; pp 101−108.

(29) Friebe, M.; Mahmood, A.; Spies, H.; Berger, R.; Johannsen, B.; Mohammed, A.; Eisenhut, M.; Bolzati, C.; Davison, A.; Jones, A. G. '3+1' Mixed-Ligand Oxotechnetium(V) Complexes with Affinity for Melanoma: Synthesis and Evaluation in Vitro and in Vivo. *J. Med. Chem.* **2000**, *43*, 2745−2752.

(30) Syhre, R.; Seifert, S.; Spies, H.; Gupta, A.; Johannsen, B. Stability versus Reactivity of "3+1" Mixed-Ligand Technetium-99m Complexes in Vitro and in Vivo. *Eur. J. Nucl. Med.* **1998**, *25*, 793−796.

(31) Mahmood, A.; Wolff, J. A.; Davison, A.; Jones, A. G. Technetium and Rhenium Complexes of Amine Amide Dithiol Ligands: Ligand Synthesis and Metal Complexes. In *Technetium, Rhenium and Other Metals in Chemistry and Nuclear Medicine 4*; Nicolini, M., Bandoli, G., Mazzi, U., Eds.; Servizi Grafici Editoriali: Padova, 1995; pp 211−215.

(32) Mahmood, A.; Kuchma, M. H.; Freiberg, E.; Goldstone, J.; Davison, A.; Jones, A. G. Functionalized Tetradentate N_2S_2 Chelates and Their Technetium-99 and Rhenium Complexes: Synthesis, Spectroscopy and Structural Characterization. In *Technetium, Rhenium and Other Metals in Chemistry and Nuclear Medicine 5*; Nicolini, M., Mazzi, U., Eds.; Servizi Grafici Editoriali: Padova, 1999; pp 253−257.

(33) Lever, S. Z.; Baidoo, K. E.; Mahmood, A. Structural Proof of *Syn*/*Anti* Isomerism in N−Alkylated Diaminedithiol (DADT) Complexes of Technetium. *Inorg. Chim. Acta* **1990**, *176*, 183−184.

(34) Francesconi, L. C.; Graczyk, G.; Wehrli, S.; Shaikh, S. N.; McClinton, D.; Liu, S.; Zubieta, J.; Kung, H. F. Synthesis and Characterization of Neutral $M^{V}O$ (M = Tc, Re) Amine−Thiol Complexes Containing a Pendant Phenylpiperidine Group. *Inorg. Chem.* **1993**, *32*, 3114−3124.

(35) O'Neil, J. P.; Wilson, S. R.; Katzenellenbogen, J. A. Preparation and Structural Characterization of Monoamine−Monoamide Bis(Thiol) Oxo Complexes of Technetium(V) and Rhenium(V). *Inorg. Chem.* **1994**, *33*, 319−323.

(36) Pelecanou, M.; Chryssou, K.; Stassinopoulou, C. I. Trends in NMR Chemical Shifts and Ligand Mobility of TcO(V) and ReO-(V) Complexes with Aminothiols. *J. Inorg. Biochem.* **2000**, *79*, 347−351.

(37) Braumann, T.; Grimme, L. H. Determination of Hydrophobic Parameters for Pyridazinone Herbicides by Liquid−Liquid Partition and Reversed-Phase High-Performance Liquid Chromatography. *J. Chromatogr.* **1981**, *206*, 7−15.

(38) Stylli, C.; Theobald, A. E. Determination of Ionization Constants of Radiopharmaceuticals in Mixed Solvents by HPLC. *Appl. Radiat. Isot.* **1987**, *38*, 701−708.

(39) (a) Johannsen, B.; Scheunemann, M.; Spies, H.; Brust, P.; Wober, J.; Syhre, R.; Pietzsch, H.-J. Technetium(V) and Rhenium(V) Complexes for 5-HT_{2A} Serotonin Receptor Binding: Structure−Affinity Considerations. *Nucl. Med. Biol.* **1996**, *23*, 429−438. (b) Johannsen, B.; Berger, R.; Brust, P.; Pietzsch, H.-J.; Scheunemann, M.; Seifert, S.; Spies, H.; Syhre, R. Structural Modification of Receptor-Binding Technetium-99m Complexes in Order to Improve Brain Uptake. *Eur. J. Nucl. Med.* **1997**, *24*, 316−319.

(40) Bowen, W. D.; de Costa, B. R.; Hellewell, S. B.; Walker, J. M.; Rice, K. C. [^{3}H]-(+)-Pentazocine: A Potent and Highly Selective Benzomorphan-Based Probe for Sigma-1 Receptors. *Mol. Neuropharmacol.* **1993**, *3*, 117−126.

(41) Hellewell, S. B.; Bruce A.; Feinstein, G.; Orringer, J.; Williams, W.; Bowen, W. D. Rat Liver and Kidney Contain High Densities of σ_1 and σ_2 Receptors: Characterization by Ligand Binding and Photoaffinity Labeling. *Eur. J. Pharmacol.-Mol. Pharmacol. Sect.* **1994**, *268*, 9−18.

(42) Vilner, B. J.; de Costa, B. R.; Bowen, W. D. Cytotoxic Effects of Sigma Ligands: Sigma Receptor-Mediated Alterations in Cellular Morphology and Viability. *J. Neurosci.* **1995**, *15*, 117−134.

(43) Brent, P. J.; Pang, G. T. σ Binding Site Ligands Inhibit Cell Proliferation in Mammary and Colon Carcinoma Cell Lines and Melanoma Cells in Culture. *Eur. J. Pharmacol.* **1995**, *278*, 151−160.

(44) (a) El Tayer, N.; van der Waterbeemd, H.; Testa, B. Lipophilicity Measurements of Protonated Basic Compounds by Reversed-Phase High-Performance Liquid Chromatography. II. Procedure for the Determination of a Lipophilic Index Measured by Reversed-Phase High Performance Liquid Chromatography. *J. Chromatogr.* **1985**, *320*, 305−312. (b) Minick, D. J.; Frenz, J. H.; Patrick, M. A.; Brent, D. A. A Comprehensive Method for Determining Hydrophobicity Constants by Reversed-Phase High-Performance Liquid Chromatography. *J. Med. Chem.* **1988**, *31*, 1923−1933.

(45) Cheng, Y.; Prusoff, W. H. Relationship between the Inhibition Constant (K_I) and the Concentration of Inhibitor Which Causes 50 Per Cent Inhibition (I_{50}) of an Enzymatic Reaction. *Biochem. Pharmacol.* **1973**, *22*, 3099−3108.

JM0005407